BMJ Open Diabetes Research & Care

Pancreatic GLP-1r binding potential is reduced in insulin-resistant pigs

Charles-Henri Malbert ,[1] Alain Chauvin,[2] Michael Horowitz,[3] Karen L Jones[3]

To cite: Malbert C-H, Chauvin A, Horowitz M, *et al*. Pancreatic GLP-1r binding potential is reduced in insulin-resistant pigs. *BMJ Open Diab Res Care* 2020;**8**:e001540. doi:10.1136/bmjdrc-2020-001540

Received 12 May 2020
Revised 11 September 2020
Accepted 23 September 2020

ABSTRACT

Introduction The insulinotropic capacity of exogenous glucagon like peptide-1 (GLP-1) is reduced in type 2 diabetes and the insulin-resistant obese. We have tested the hypothesis that this response is the consequence of a reduced pancreatic GLP-1 receptor (GLP-1r) density in insulin-resistant obese animals.

Research design and methods GLP-1r density was measured in lean and insulin-resistant adult miniature pigs after the administration of a ^{68}Ga-labeled GLP-1r agonist. The effect of hyperinsulinemia on GLP-1r was assessed using sequential positron emission tomography (PET), both in the fasted state and during a clamp. The impact of tissue perfusion, which could account for changes in GLP-1r agonist uptake, was also investigated using ^{68}Ga-DOTA imaging.

Results GLP-1r binding potential in the obese pancreas was reduced by 75% compared with lean animals. Similar reductions were evident for fat tissue, but not for the duodenum. In the lean group, induced hyperinsulinemia reduced pancreatic GLP-1r density to a level comparable with that of the obese group. The reduction in blood to tissue transfer of the GLP-1r ligand paralleled that of tissue perfusion estimated using ^{68}Ga-DOTA.

Conclusions These observations establish that a reduction in abdominal tissue perfusion and a lower GLP-1r density account for the diminished insulinotropic effect of GLP-1 agonists in type 2 diabetes.

Significance of this study

What is already known about this subject?

- The insulinotropic capacity of exogenous glucagon like peptide-1 (GLP-1) is reduced in type 2 diabetes and the insulin-resistant obese.
- A reduced efficacy of GLP-1 receptor (GLP-1r) agonists could be related to a downregulation of GLP-1r, particularly given that plasma levels of endogenous GLP-1 are normal in insulin-resistant obese.

What are the new findings?

- GLP-1r binding potential in the obese pancreas is reduced by 75% compared with lean animals.
- Duodenal GLP-1r is not downregulated in obese insulin-resistant animals.
- Induced hyperinsulinemia reduces pancreatic GLP-1r density in lean, but not obese, animals.

How might these results change the focus of research or clinical practice?

- The reduction in pancreatic GLP-1r may contribute to the variability in the clinical response to GLP-1r agonists observed in type 2 diabetes.
- The capacity to investigate non-invasively GLP-1r may be of relevance to a more personalized therapeutical approach.

INTRODUCTION

Observations that the insulinotropic capacity of exogenous glucagon like peptide-1 (GLP-1) is reduced, but preserved, in type 2 diabetes and the insulin-resistant obese[1] while that of GIP is markedly attenuated provided the stimulus for the development of 'GLP-1 based' treatment for type 2 diabetes. In these patients, GLP-1 receptor (GLP-1r) agonists and DDP-4 inhibitors are effective in reducing elevated glucose levels.[2] While most patients respond to GLP-1r agonists and DDP-4 inhibitors, there is a substantial interindividual variation in the response,[3] and many patients do not achieve the target HbA1c of ≤7%. With some rare exceptions, no clear factors have hitherto been identified to indicate which patients will respond best to these drugs, with the predictable exception that the reduction in HbA1c is greater when baseline HbA1c is higher.[4] One hypothesis to account for a reduced efficacy of GLP-1r agonists is downregulation of GLP-1, particularly given that it is generally accepted that plasma levels of endogenous GLP-1 are normal.[5] Moreover, there is evidence for GLP-1r downregulation in several tissues and organs. A reduction in mRNA GLP-1r levels in gastric glands type 2 diabetes has been reported,[6] and downregulation of vascular GLP-1r expression has been demonstrated in obese subjects without diabetes.[7] It has also been reported that GLP-1r expression in visceral adipose tissue is inversely correlated with weight in obese subjects[8] while, surprisingly, the converse, that is, an increased expression, has been observed in insulin-resistant obese.[9] GLP-1r regulation in the pancreas has not been evaluated adequately. It has been suggested that chronic hyperglycemia was responsible for the reported downregulation of GLP-1r in a partial pancreatectomy model in the rat.[10] However, the reported downregulation may well reflect

[1]Aniscan Unit, Department of Human Nutrition, INRAE, Saint-Gilles, France
[2]UEPR Unit, Department of Animal Physiology, INRAE, Saint-Gilles, France
[3]Center of Research Excellence in Translating Nutritional Science to Good Health, The University of Adelaide, Adelaide, South Australia, Australia

Correspondence to
Dr Charles-Henri Malbert;
charles-henri.malbert@inrae.fr

the inherent limitations of GLP-1r expression data generated through the use of antibodies or the final autoradiography step that severely limits the resolution of the output signal.[11] These issues have recently been overcome by the availability of in vivo radio-labeled probes suitable for competition studies.[12] Specifically, the recent achievement of the Eriksson team in labeling a GLP-1r agonist with a positron emitter,[12] while targeted towards the detection of insulinomas, provides the capacity to quantify the GLP-1r non-invasively. This was made possible by the design of the extemporaneous synthesis sequence of a ^{68}Ga-labeled exendin-4 tracer and its companion quality control process.[13] This approach is minimally invasive, supersedes non-quantitative histological techniques using suboptimal antibodies,[11] and allows the simultaneous investigation of the GLP-1r in key glucose homeostatic abdominal organs under different experimental conditions.

The primary aim of our work was to test the hypothesis, in vivo, that pancreatic GLP-1r binding potential is reduced in obese insulin-resistant animals. Using the unique capability of [^{68}Ga]Ga-DO3A-VS-Cys40-exendin-4 to image GLP-1r within the entire abdominal cavity, we have quantified this reduction in an organ-dependent manner. Since a reduction in GLP-1r binding potential could also be the consequence of hyperglycemia[10] and/or hyperinsulinemia,[14] we determined the effect of hyperinsulinemia during euglycemia by administration of a GLP-1r radioactive agonist during the plateau of a euglycemic–hyperinsulinemic clamp in both lean and obese animals. ^{68}Ga-DOTA[15] distribution was used concomitantly to quantify blood flow, which could affect the binding potential without altering receptor affinity.[16] We performed our experiments in miniature obese and lean Yucatan adult pigs in whom relative spatial resolution is higher even when compared with that obtained in rats using a dedicated miniature positron emission tomography (PET) imager.[17] Furthermore, extensive agonist displacement studies have been performed in this species to ascertain the specific binding of the radioactive probe.[18] Finally, the mini-pig is known to develop obesity and insulin resistance rapidly in response to a high-fat/high-sucrose diet,[19] and euglycemic clamp steady-state conditions can be maintained for extended periods.[20]

MATERIALS AND METHODS

Experimental protocol

A total of 14 adult Yucatan mini-pigs (INRA, Saint-Gilles, France), matched for age and sex, were used. At 1 year of age, seven animals were made obese using a high-fat, high-sucrose diet (4.024 kcal/kg feed, 14.1% unsaturated fat, and 6.4% sucrose expressed in % dry matter) supplied at 150% of the recommended caloric intake for 5 months to induce morbid obesity.[20] The remaining seven animals were maintained on a low-fat, low-sucrose diet (2.275 kcal/kg feed, 4.1% unsaturated fat, and 3.5% sucrose expressed in % dry matter) for 5 months to limit body fat and ensure that total body weight was less than 40 kg. Immediately after this time, and while animals were provided with the same feeding regimen, PET-CT imaging of the abdominal area, using a GLP-1r PET radiotracer, was performed. Adiposity was measured using CT imaging of the abdomen.[21] Four hours after administration of the GLP-1r radiotracer, and while the animal was still anesthetized, a second session of PET-CT was performed to evaluate the abdominal blood flow using ^{68}Ga-DOTA. Between 3 and 4 weeks later, when the animals had recovered, insulin sensitivity was measured using a euglycemic–hyperinsulinemic clamp.[20] The insulin sensitivity index was calculated according to Malbert *et al*.[22] While the clamp was at its plateau phase, GLP-1r PET imaging was again performed to evaluate the impact of hyperinsulinemia on the GLP-1r binding potential. In the interval between the procedures, the animals were housed individually in 2 m^2 cages, enriched with toys to encourage physical exercise. Visual and limited physical contact between animals was permitted by the design of the cages. Animals were euthanized using T61 (Intervet, France) at the end of the last PET imaging sequence.

GLP-1r PET imaging

GLP-1r was labeled using [^{68}Ga]Ga-DO3A-VS-Cys40-exendin-4 produced on-site using an automated workflow, according to Velikyan *et al*[13 23] adapted for a Scintomics radioactive synthesizer. Briefly, ^{68}Ga was produced daily by automatic elution of a chemical grade generator (iThema Labs, DSD-Pharma, Austria) with 6 mL 0.6 M HCl Suprapure (ABX, HCL-101) as part of the synthesis process. During the period when experiments were conducted, the generator was eluted daily to maintain the capacity of the tin dioxide polyethylene column to retain ^{68}Ge from the eluate. Production of [^{68}Ga]Ga-DO3A-VS-Cys40-exendin-4 was achieved using a ^{68}Ga-peptide synthesis cassette (ABX Scintomics, SC-1, Germany) with 47 µg of the DO3A-VS-Cys40-Exendin-4 cold molecule (CSBio peptide, USA) dissolved in 2.5 mL Hepes buffer (Sigma, France) inserted in the reactor. The synthesizer sequence (Scintomics GRP, Germany) was modified to (1) adjust for the temperature and heating duration of the reactor, (2) allow for extended tubing between the reactor and the final vial containing the radioactive compound, and (3) reduce the volume of phosphate buffer from 15 to 5 mL as a consequence of the final filtration step removal without affecting the final pH (pH=7.4). Prior to injection, the final compound was checked using high-performance chromatography for the amount of ^{68}Ga that was not associated with exendin-4 and the concentration of exendin-4 labeled by ^{68}Ga in solution.[23]

PET images were acquired during isoflurane anesthesia using a Discovery ST PET-CT scanner (GE, France). The animals were anesthetized with isoflurane (measured minimum alveolar concentration 1.8 vol) in an air/O_2 mixture. The ventilation parameters were set to maintain $spCO_2$ at 4.3%±2% and spO_2 at 98%, or more, while the insufflation pressure was less than 20 mm Hg (ADU-AS/3; GE). Homeothermy was maintained using a forced hot-air blanket (Bair Hugger; 3M, France). Immediately before the imaging, access to arterial blood was achieved with a

Seldinger-type catheter (RS+A50K10SQ,; Terumo, France) inserted extemporaneously under echographic guidance (M Turbo; Sonosite, France) into either the left or right femoral artery. A venous catheter was also placed in one of the saphenous veins contralateral to the arterial catheter. These catheters were interconnected to establish the artery-venous loop used to calculate the arterial input function during the imaging sequence. Each animal was positioned to include the abdomen in the 15 cm axial field of view of a Discovery ST PET/CT scanner (GE Healthcare) with the assistance of a low-dose CT scout view (140 kV, 10 mAs). Attenuation correction was performed using a CT examination at 140 kV and 10–80 mA. ^{68}Ga-DO3A-exendin-4 (0.2 MBq/kg) was administered intravenously over 30 s using an automated injector, and animals were examined with a dynamic PET protocol for 60 min (30 frames; 12×10 s, 6×30 s, 5×120 s, 5×300 s, and 2×600 s). Concurrent with the PET scanning, arterial blood radioactivity was recorded continuously using an in-line device coupled with a gamma-ray detector (Model 802 Canberra; Areva, France) placed on the external artery-venous loop. Blood was drawn from the artery and re-injected into the vein at a rate of 8.0±0.1 mL/min through a peristaltic pump controlled by an artificial intelligence algorithm (Labview 17, USA), receiving the flow signal from a transit-time ultrasonic probe clipped onto the loop tubing (Transonic; Emka Technologies, France). Arterial blood was also sampled at 10 min intervals with a blood sampler (Instech; Phymep, France) connected to the loop after the radioactivity probe. The radioactivity of whole blood and plasma samples was measured using a gamma counter (Wizard 1470; Perkin Elmer, France). Data originating from the in-line blood sampler were corrected for dispersion caused by the length of the arterial sampling line, according to Munk *et al*.[24] Composite arterial input function was built from these measurements using AniMate software.[25]

GLP-1r binding potentials were obtained for the pancreas, the duodenum, and the abdominal fat using compartmental kinetic analysis of the radioactivity in the abdominal organ's volume of interest (VOI) with the arterial input function after corrections for attenuation, scatter, dead time, and partial volume effect. Briefly, PET images were reconstructed using an iterative OSEM algorithm (3D iterative, 4 mm Hann filter, two iterations/21 subsets) into a 128×128 matrix with pixel size 2.34×2.34×3.27 mm. Once reconstructed and time-averaged, these were used, together with CT images, to build semi-automatically VOI of the abdominal organs using ITK-Snap software. Reconstructed data were analyzed using PMod V.3.9 (Pmod, Switzerland) that was also used for partial volume correction.[26] Data were fitted to a two-tissue compartment model with Akaike and Bayesian information criteria (unitless) as an indicator of the adequacy of the model compared with a one-tissue model. The compound parameter Vs (specific volume of distribution) describes the binding potential.[27] PET images were also converted and coded, voxel-wise, in units of binding potential (mL/ccm) using Logan plot for representation purposes. The GLP-1r binding potential was not calculated for the liver or the spleen since there was no GLP-1r signal in these organs.[28]

^{68}Ga-DOTA imaging

Visceral blood flow was quantified using ^{68}Ga-DOTA injected during the first PET-CT imaging session, at least 5 hours after the injection of the GLP-1r radioactive compound while the animal was still anesthetized. ^{68}Ga-DOTA was synthesized using a custom-made cassette adapted for a Scintomics radioactive synthesizer. The synthesis process was adapted from Velasco *et al*[29] and Autio *et al*[30] and incorporated a software trigger associated with a radioactive sensor to discard early and late elution segments of the ^{68}Ga generator. The final product was analyzed for radionuclide purity by iTLC using a linear radioactivity reader (Scan-RAM; LabLogic, UK). ^{68}Ga-DOTA solution was spotted on a iTLC-SG activated paper (Agilent, USA) with either 1 M ammonium acetate/methanol (1:1) or 0.1 M citrate buffer as mobile phase[31] with revelation times of 15 and 5 min, respectively. Retention times and areas under the curve were calculated using Laura software (LabLogic).

PET images and arterial input functions were obtained using the same set-up as described for GLP-1r imaging. ^{68}Ga-DOTA (1.2 MBq/kg) was administered intravenously over 10 s using an automated injector and animals were examined with a dynamic PET protocol for 10 min (46 consecutive frames—30×5 s, 6×10 s, 3×20 s, 4×30 s, and 3×60 s). Image reconstruction was performed as described earlier including partial volume correction irrespective of the size of the VOI.

K1, the unidirectional transfer rate from blood to tissue obtained from the iterative fitting of PET and arterial input data to a one-tissue compartment model (Pmod), was used to quantify visceral blood flow.[32]

Phenotypic parameters

The CT images (Discovery ST; General Electric Medical Systems, France) were used to quantify subcutaneous and abdominal fat volumes.[33] Segmentation of subcutaneous and intra-abdominal fat was performed semi-automatically using ITK-Snap. Total abdominal fat was estimated as the sum of subcutaneous and intra-abdominal fat.[23] Hepatic[34] and pancreatic[35] fat were estimated as the ratio of X-ray attenuations between the organ and the spleen, which was used as a reference tissue. The VOIs applied for PET quantification were also used for attenuation measurement. Hepatic fat was estimated in percentage of fat using published correlation data.[36]

Insulin sensitivity was measured using a euglycemic–hyperinsulinemic clamp performed before the second PET imaging procedure. Insulin (Actrapid; Novo Nordisk, Denmark) and 20% glucose were infused into the saphenous vein. Insulin was diluted in 50 mL saline plus 0.5% homologous blood and infused at 120 mU kg^{-1} h^{-1} without a priming dose. Arterial blood samples were obtained from the femoral artery every 5 min and

measured by the glucose oxidase method on a rapid analyzer (GM9 Analyzer; Analox Instruments, UK). In each clamp, the plateau was considered to have been achieved when differences in glucose uptake rate and glycemia were less than 5% in three consecutive samples. Plasma insulin concentrations were measured using a ST-AIA-Pack IRI reagent kit, with a quantification limit of 0.5 µU/mL and intra-assay coefficient of variation less than 2% from 12 to 200 µU/mL.

Statistical analysis

Data are presented as mean±SEM and were compared using an unpaired t-test with Prism 8 (GraphPad Software, USA). Differences were considered statistically significant if p value ≤0.05.

RESULTS

Phenotypic characterization

In all animals in the obese group, body weight doubled approximately, mainly as a consequence of an increase in abdominal fat mass that was about six times than that in the lean group. The abdominal fattening was partially the consequence of an increase in visceral fat, but the dominant increase was in subcutaneous fat. An increase in fat mass was also evident in the liver and the pancreas, and there was a significant decrease of the liver/spleen and pancreas/spleen ratio (figure 1). The latter was of the same order as that of the abdominal fattening. Mean fasting plasma glycemia was slightly, although not significantly, higher in the obese compared with the lean group. Basal insulinemia in the obese, measured before the onset of the clamp, was about three times that of lean animals. In obese animals, the amount of metabolized glucose during the euglycemic–hyperinsulinemic clamp was about 50% that of lean animals. As a consequence, the calculated insulin sensitivity index was reduced by about 70%.

Distribution volume of specific binding in lean and obese

The binding potential, expressed as the distribution volume of specific binding (Vs) was significantly decreased in obese compared with lean animals for the pancreas, as well as subcutaneous and visceral fat (figure 2, table 1). In contrast, there was no change in duodenal binding potential despite the adequate fit to a two-tissue compartment model as demonstrated by Akaike information criteria that were not significantly different from those obtained collectively for the pancreas and the abdominal fat (38±10 vs 42±13, respectively, unitless, p>0.05). Similarly, the uptake in the duodenum was not affected by obesity status (figure 3). The changes in radioactivity obtained from the gastric VOI could not be fitted to a two-tissue compartment model while maintaining a realistic error, and gastric GLP-1r uptake was, accordingly, not taken into account in subsequent analyses.

The value of K1, which determines total tissue uptake (free, specific, and non-specific) from plasma, was markedly reduced in the obese compared with the lean animals for both the pancreas and the abdominal fat tissues. In contrast, K1 was significantly increased in the duodenum in obese animals (figure 4). The individual rate constant k3, regarded as the rate of association of the ligand with the specific binding sites, was significantly decreased in both the pancreas and the subcutaneous fat in the obese animals. No significant changes were evident for the k3 value in either the duodenum or the visceral fat.

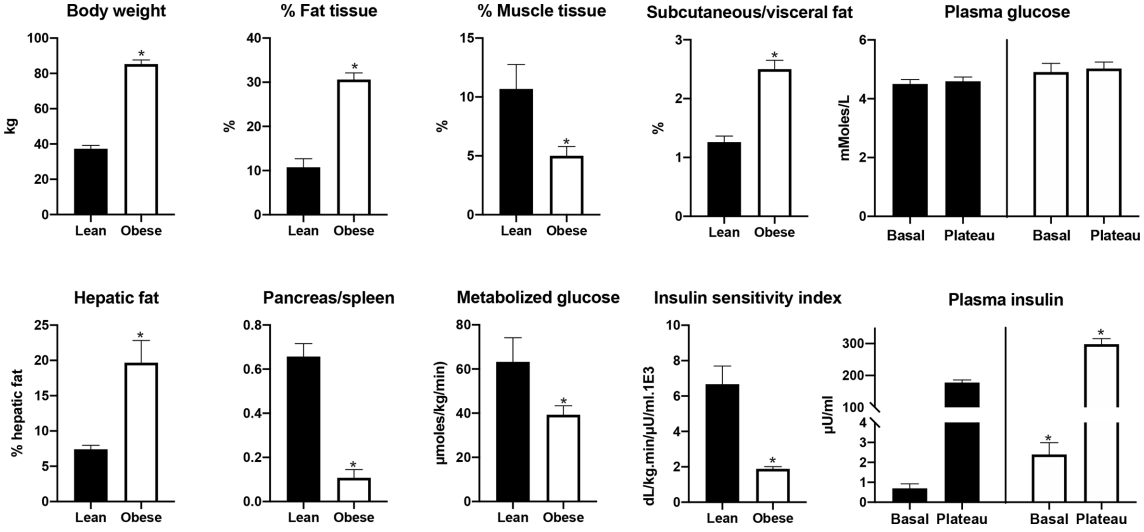

Figure 1 Differences in phenotypic and metabolic features between the lean and obese groups. Note the absence of hyperglycemia in the obese while the fasting insulin is already elevated. Fat and muscle tissue percentage and the ratio between subcutaneous and visceral fat were quantified using a CT image of the abdomen. Hepatic fat was calculated from the ratio of X-ray attenuation between the liver and the spleen. Fat infiltration in the pancreas was estimated using the same method, but in the absence of a published correlation is presented only as ratio between the two attenuations. Metabolized glucose and insulin sensitivity were calculated from the clamp data. *Indicates a significant difference at p<0.05 between groups.

Table 1 GLP-1r binding potential expressed as a distribution volume of specific binding (Vs expressed in mL/ccm) obtained after fitting of the [^{68}Ga]Ga-DO3A-VS-Cys40-exendin-4 uptake to a 2-tissue compartment model in both the fasted state and during the plateau phase of a hyperinsulinemic–euglycemic clamp

	Lean		Obese	
	Fasted	Insulin	Fasted	Insulin
Pancreas	4.54±0.35	1.61±0.45*	1.49±0.47†	1.54±1.31
Duodenum	3.02±0.20	2.62±0.17	2.87±0.29	2.88±0.25
Subcutaneous fat	0.13±0.02	0.09±0.02*	0.06±0.02†	0.08±0.03
Visceral fat	0.44±0.13	0.17±0.02*	0.13±0.02†	0.08±0.03

*Difference between fasted and insulin condition in lean animals.
†Difference between lean and obese animals.
GLP-1r, glucagon like peptide-1 receptor; Vs, specific volume of distribution.

^{68}Ga-DOTA uptake

K1 values obtained after the injection of ^{68}Ga-DOTA confirmed the reduction in perfusion observed for the pancreas and the subcutaneous fat in the obese compared with lean animals. The magnitude of this reduction at the pancreatic level was almost sufficient to suppress K1 expression in the parametric abdominal images (figure 5). No significant changes were observed for visceral fat between the two groups (table 2). Duodenal perfusion, unlike that of other abdominal organs, was increased (about double) in obese versus lean animals.

Insulin-induced changes in Vs

Exogenous administration of insulin reduced pancreatic and abdominal fat volumes of specific binding in the lean animals to values comparable with those in the obese group (both with and without the clamp). The plasma glucose was essentially identical to the fasting condition during the euglycemic–hyperinsulinemic clamp procedure, but the insulinemia was much greater, both during fasting and the clamp, in the obese compared with lean animals (see figure 1). The reduced Vs during the clamp in the lean animals reflected a reduction in the K1 and k3 values. Since K1 in the two-tissue compartment model is a compound parameter, and in the absence of K1 value obtained from ^{68}Ga-DOTA during a clamp, it is not possible to ascertain that this reduction reflected a parallel decrease in tissue perfusion. In the obese group, there was no change in the GLP-1r transfer coefficients between the fasting and clamp conditions. Furthermore, the uptake curves between these conditions were comparable, indicating that insulin did not affect GLP-1r uptake in obese animals.

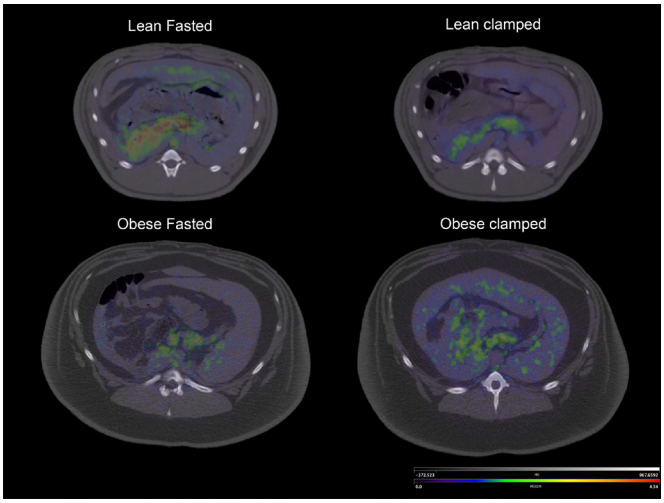

Figure 2 Hybrid image representing Vs (binding potential) coded PET image over CT anatomical image. Note the clear uptake of the GLP-1r radiolabel in the lean fasted animal and the reduction in Vs during clamp. This Vs value was similar to that observed in the obese animal both in the fasted condition and during the clamp. The scale was identical between the four conditions. Vs images were calculated using the Logan graphical method. GLP-1r, glucagon like peptide-1 receptor; Vs, specific volume of distribution.

DISCUSSION

Capitalizing on the recent capacity to quantify GLP-1r using PET non-invasive imaging, we demonstrated in an animal model of obesity exhibiting insulin resistance that obesity is associated with a marked reduction in GLP-1r binding potential in the pancreas, as well as visceral and subcutaneous fat, but not in the duodenum. The reduction in pancreatic GLP-1 binding appears to reflect both a decrease in organ perfusion, as demonstrated by a reduction in ^{68}Ga-DOTA uptake, and a diminished rate of association of the ligand with the specific binding sites. Furthermore, these phenomena were replicated, in lean animals, by an acute increase in plasma insulin during euglycemia. Collectively, these observations support the concept that the abdominal GLP-1r downregulation is important in the pathophysiology of insulin-resistant obesity.

Resistance to the insulinotropic effect of GLP-1r may potentially account for the relative reduction in the effect of exogenous GLP-1 and GLP-1 agonists in insulin-resistant obese and in type 2 diabetes[5] as well as the substantial interindividual variability in the glucose-lowering response to GLP-1r agonists.[37] A reduction in GLP-1r in the vagal nodose ganglion,[38] in β (and probably α) pancreatic cells,[10] in endothelial cells,[7] and in gastric glands[6] have been reported. In all but one of

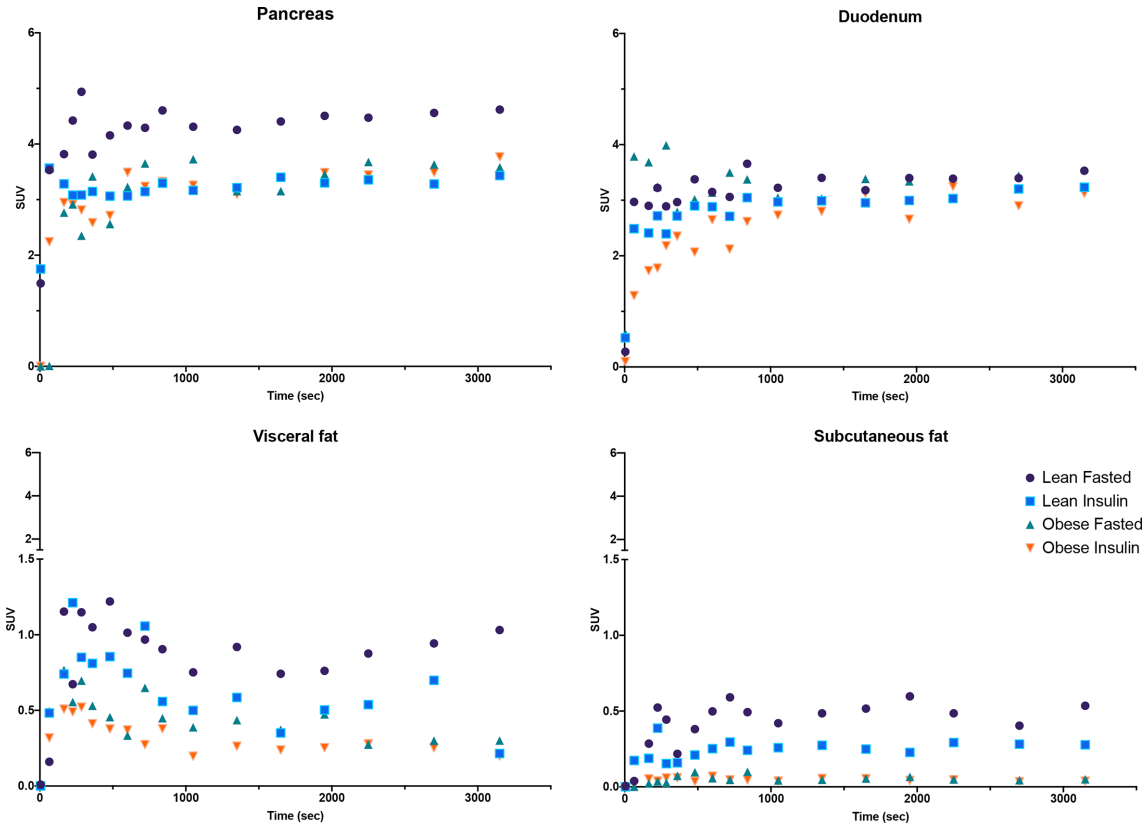

Figure 3 Time activity curves describing [^{68}Ga]Ga-DO3A-exendin-4 uptake in the pancreas, duodenum, visceral, and subcutaneous fat for fasting and clamp conditions in lean and obese animals. For simplicity, SE and several time intervals at the beginning of the curves are not presented. The uptake by the stomach is also not presented since it does not follow a 2-tissue compartment model. Note the absence of an effect of obesity and/or of hyperinsulinemia produced by the clamp on duodenal uptake, while obesity and hyperglycemia both reduce it. SUV, standard uptake value.

these studies, data were derived from quantitative in vitro expression of RNA, and the etiology of this was not investigated. Xu *et al*,[10] using a 4-day-long hyperglycemic clamp, reported that the downregulation of pancreatic GLP-1r observed in the partially pancreatectomized rat was the consequence of hyperglycemia. While our data were obtained in insulin-resistant, but not diabetic, pigs, they argue against the concept that GLP-1r downregulation is the consequence of hyperglycemia alone in that reduction as the binding potential induced in lean subjects by a hyperinsulinemic–euglycemic clamp was of comparable magnitude with that observed in obese animals.

A striking observation was the absence of an impact of obesity on the expression of duodenal GLP-1r. That the stability in duodenal binding potential clearly paralleled the stability of the k3 transfer parameter indicates that this feature is unlikely to represent the outcome of an experimental error. Both the Akaike information criteria, together with the fitting error, fell well within accepted criteria. The unaltered duodenal binding potential was also not the consequence of a low GLP-1r density since the latter was within the same range as that observed in the pancreas of both lean and obese animals. Duodenal GLP-1r is known to be functional since duodenal GLP-1 signaling regulates hepatic glucose production[39] and induces barrier protective expression in Brunner's glands[40] in rats. Finally, the radioligand is likely to reach the binding site of the duodenal receptor since the cold compound given in a pharmacologic dose induces an effect identical to that of GLP-1.[39] It is possible that the use of isoflurane for anesthesia in our studies may have an impact of insulin secretion and glucose utilization.[41] This might explain, in part, the absence of an impact of obesity on duodenal GLP-1r. While we do not have a clear explanation to account for the duodenal GLP-1r behavior, it might contribute to the slowing of gastric emptying induced by exogenous GLP-1 and GLP-1r agonists in both healthy subjects and patients with type 2 diabetes[33] by inhibition of duodenal motility.[4 42]

A reduction in tissue perfusion is an important, although not exclusive, contributor to the lower binding potential in obese animals, as demonstrated by a paralleled decrease in K1 obtained from ^{68}Ga-DO3A-exendin-4 and ^{68}Ga-DOTA analysis. For example, at the pancreatic level, K1 obtained from GLP-1r images was reduced by about 80%, while the reduction was about 90% for the flow-coded images. While conclusive information about the relation between blood flow and pancreatic β-cell function is lacking, impaired pancreatic blood flow was identified as a major contributor to reduced pancreatic energy metabolism measured by ^{18}FDG imaging in morbidly obese humans.[43] Furthermore, the reduction in

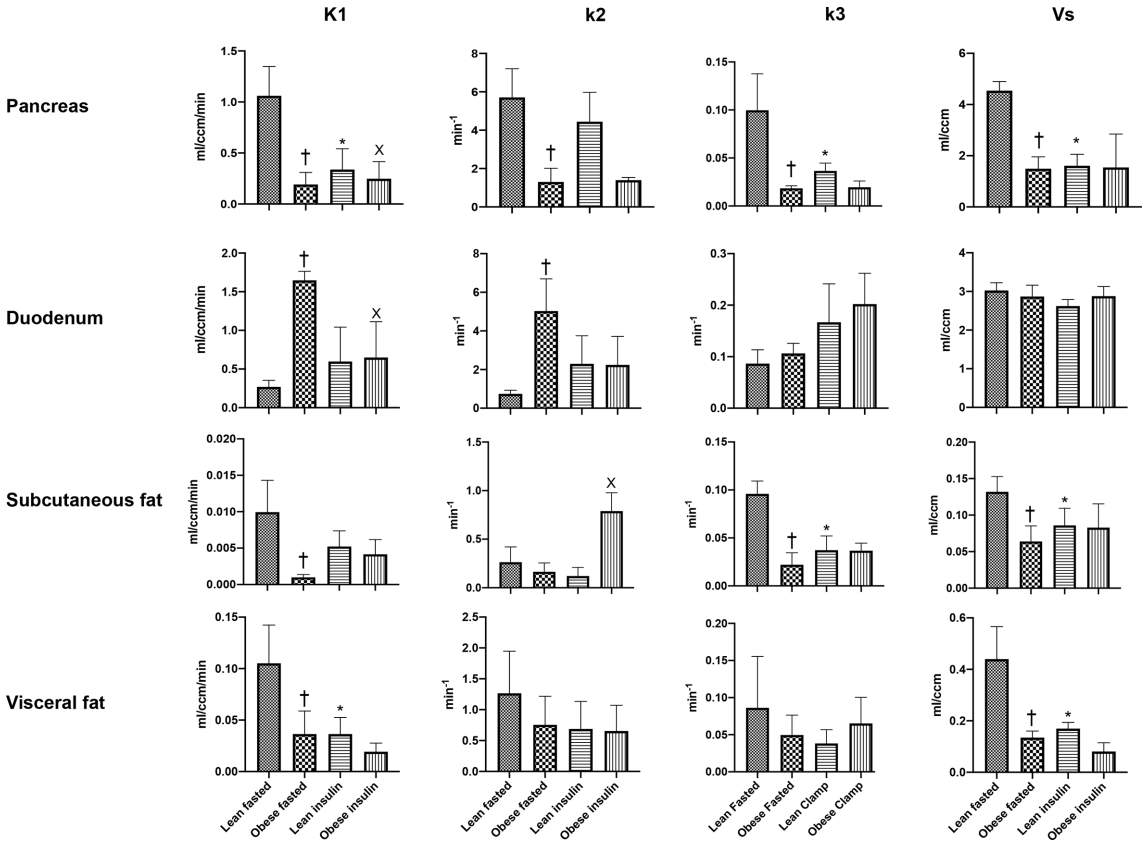

Figure 4 Transfer parameters of the 2-tissue compartment model describing the tissue uptake of [^{68}Ga]Ga-DO3A-exendin-4. The value of the binding potential is also presented as Vs value. Note that all tissues, with the exception of the duodenum, exhibit a reduction in K1 as a consequence of obesity, a feature reproduced in lean animals by the administration of exogenous insulin. The same evolution is also evident for k3 parameter representing the rate of association of the ligand with the specific binding sites. †Significant difference from lean fasted, *significant difference from lean fasted, X significant difference from obese fasted. Vs, specific volume of distribution.

blood flow was associated with concomitant reductions in β-cell glucose sensitivity, insulinogenic index, and incremental glucose during an oral glucose tolerance test.[43] We do not have access to a cyclotron in line with our PET and substituted the classical [^{15}O]H_2O flow tracer to ^{68}Ga-DOTA which has not been validated for abdominal organ perfusion. While it is effective in measurement of the perfusion of the heart[15] and lung,[30] the properties of this tracer could account for the substantial reduction in K1 compared with the more modest impairment reported in obese versus lean patients using the [^{15}O]H_2O method. Similarly, this may explain why the reported perfusion of abdominal fat in animals and humans was reduced.[44]

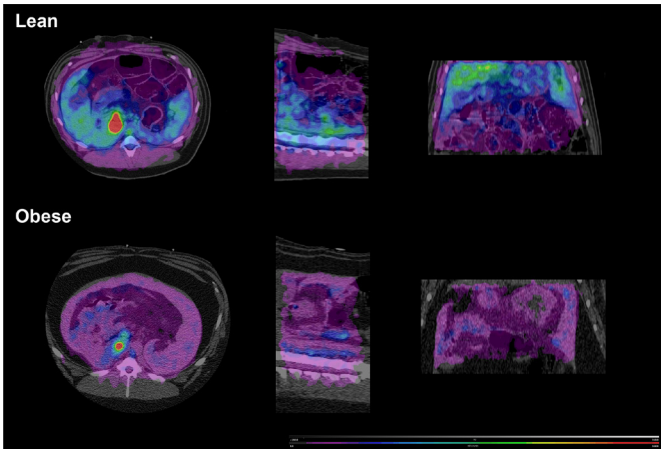

Figure 5 Hybrid image representing K1 coded PET image of ^{68}Ga-DOTA distribution over CT anatomical image. The PET image was coded pixel-wise for K1 then filtered with a Gaussian filter for presentation. Note that K1 was markedly reduced in the obese demonstrating an overall reduction in tissue perfusion for both the duodenum and the pancreas.

Table 2 K1 values (in mL ccm^{-1} min^{-1}) derived from ^{68}Ga-DOTA uptake after adjustment of the distribution to a 1-tissue compartment model

	Lean	Obese
Pancreas	1.57±0.67	0.14±0.05*
Duodenum	0.14±0.02	0.40±0.21*
Subcutaneous fat	0.08±0.03	0.01±0.01*
Visceral fat	0.02±0.01	0.03±0.01

K1 values were representative for the tissue perfusion and indicated a reduced flow for the pancreas and the subcutaneous fat in the obese animals while there was an increase in the duodenal area.
*p<0.05.

The observed capacity of GLP1-r to be downregulated in lean pigs after euglycemic intravenous glucose is important, especially as a reduced binding potential was evident for all abdominal organs with the exception of the duodenum. The reduction in GLP1-r expression could potentially be the consequence of an increase in insulinemia and/or a decrease in glucagonemia. While we did not measure plasma glucagon concentrations, hyperinsulinemia is integral to the clamp. The latter is potentiated by insulin resistance, and the glucose infusion would be anticipated to suppress glucagon secretion. Indeed, isoglycemic intravenous glucose, but not oral glucose, has been shown to decrease circulating glucagon concentrations in type 2 diabetes,[45] which has been linked to the reduced incretin effect evident in this group.[46] The relatively rapid change in binding potential observed in lean animals during the clamp support this hypothesis, at least for the GLP-1r–dependent fraction of the incretin effect.

While we conducted a true quantitative assessment of GLP-1r density using the unique capability of [^{68}Ga] Ga-DO3A-VS-Cys40-exendin-4 to bind reversibly on the GLP-1r, the method used cannot discriminate downregulation of the number of GLP-1r per unit of volume from a reduced affinity of exendin-4 towards its natural receptor. Absolute affinity could be measured quantitatively through PET measurements since affinity is the ratio between binding potential (BPf) and Bmax.[27] Similarly, our organ-based approach is unable to provide information about the cells that were expressing less GLP-1r during obesity. It is likely that the reduced GLP-1r observed in the pancreas of obese animals is not associated with β-cell expression since the ablation of these cells by streptozotocin is not associated with a reduction in pancreatic ^{68}Ga-DO3A-exendin-4 uptake in pigs.[47] Other GLP-1–1r expressing cells have been identified, including the pancreatic ductal cells and pancreatic alpha and delta cells.[48]

In conclusion, we have demonstrated that there is GLP-1r downregulation in the majority of the abdominal organs in insulin-resistant animals which is likely to relate to an increase in plasma insulin. The reduction in pancreatic GLP-1r may contribute to the inter-individual variability of the clinical response to GLP-1r agonists observed in type 2 diabetes, and the non-invasive assessment of GLP-1r may be of relevance to a more personalized therapeutical approach. In contrast, the duodenal GLP-1r was not downregulated, which may be of relevance to the gastrointestinal side effects of GLP-1r agonists, especially nausea and gastroparesis. The reason for the maintenance of duodenal GLP-1r binding potential in insulin-resistant animals and whether this is also the case in more distal parts of the gut warrant additional investigations.

Acknowledgements The authors thank staff of the UEPR unit for animal care, Mickael Genissel, Julien Georges, Francis Le Gouevec, and Vincent Piedvache. We also thank Emilie Lebrun and Laurine Picquemal for their involvements in running the administrative aspect of the Aniscan imaging facility and Raphael Comte (Pegase unit) for insulin measurements. We also acknowledge Biogenouest and Prism core facility.

Contributors C-HM planned the experiments, conducted the studies, analyzed the data, and was primarily responsible for writing the manuscript. AC conducted the studies and analyzed the data. MH and KLJ made a major contribution to the writing of the manuscript, including data interpretation. C-HM is the guarantor of this work and, as such, had full access to all the data in the study and takes responsibility for the integrity of the data and the accuracy of the data analysis.

Funding The study was conducted within the Aniscan Imaging Center (Aniscan, INRA), which is supported by BPIFrance within the Investments for the Future program. KLJ's salary is supported by the University of Adelaide William T Southcott Research Fellowship.

Competing interests None declared.

Patient consent for publication Not required.

Ethics approval The experiment was conducted according to the ethical standards of European and French legislation, and with the approval of the Rennes Animal Ethics Committee (2018053109128366).

Provenance and peer review Not commissioned; externally peer reviewed.

Data availability statement Data are available in a public, open access repository. The datasets generated and analyzed during the current study are available in the INRAE data repository (https://doi.org/10.15454/F3V6L2). The archive includes the Pmod database with raw and analyzed images in a structured format. Model analyses together with arterial input functions are also included in the data repository. The metadata associated with the archive explained how to use it.

ORCID iD

Charles-Henri Malbert http://orcid.org/0000-0002-0665-4545

REFERENCES

1 Nauck MA, Meier JJ. The incretin effect in healthy individuals and those with type 2 diabetes: physiology, pathophysiology, and response to therapeutic interventions. *Lancet Diabetes Endocrinol* 2016;4:525–36.
2 Drucker DJ. Mechanisms of action and therapeutic application of glucagon-like peptide-1. *Cell Metab* 2018;27:740–56.
3 Monami M, Dicembrini I, Nreu B, *et al*. Predictors of response to glucagon-like peptide-1 receptor agonists: a meta-analysis and systematic review of randomized controlled trials. *Acta Diabetol* 2017;54:1101–14.
4 Marathe CS, Rayner CK, Jones KL, *et al*. Relationships between gastric emptying, postprandial glycemia, and incretin hormones. *Diabetes Care* 2013;36:1396–405.
5 Gasbjerg LS, Bergmann NC, Stensen S, *et al*. Evaluation of the incretin effect in humans using GIP and GLP-1 receptor antagonists. *Peptides* 2020;125:170183.
6 Broide E, Bloch O, Ben-Yehudah G, *et al*. Reduced GLP-1R expression in gastric glands of patients with type 2 diabetes mellitus. *J Clin Endocrinol Metab* 2014;99:E1691–5.
7 Kimura T, Obata A, Shimoda M, *et al*. Down-regulation of vascular GLP-1 receptor expression in human subjects with obesity. *Sci Rep* 2018;8:10644.
8 Ejarque M, Guerrero-Pérez F, de la Morena N, *et al*. Role of adipose tissue GLP-1R expression in metabolic improvement after bariatric surgery in patients with type 2 diabetes. *Sci Rep* 2019;9:6274.
9 Vendrell J, El Bekay R, Peral B, *et al*. Study of the potential association of adipose tissue GLP-1 receptor with obesity and insulin resistance. *Endocrinology* 2011;152:4072–9.
10 Xu G, Kaneto H, Laybutt DR, *et al*. Downregulation of GLP-1 and GIP receptor expression by hyperglycemia: possible contribution to impaired incretin effects in diabetes. *Diabetes* 2007;56:1551–8.
11 Pyke C, Knudsen LB. The glucagon-like peptide-1 receptor—or not? *Endocrinology* 2013;154:4–8.

12 Selvaraju RK, Velikyan I, Asplund V, *et al*. Pre-clinical evaluation of [(68)Ga]Ga-DO3A-VS-Cys(40)-Exendin-4 for imaging of insulinoma. *Nucl Med Biol* 2014;41:471–6.
13 Velikyan I, Rosenstrom U, Eriksson O. Fully automated GMP production of [^{68}Ga]Ga-DO3A-VS-Cys^{40}-Exendin-4 for clinical use. *Am J Nucl Med Mol Imaging* 2017;7:111–25.
14 Kjems LL, Holst JJ, Vølund A, *et al*. The influence of GLP-1 on glucose-stimulated insulin secretion: effects on beta-cell sensitivity in type 2 and nondiabetic subjects. *Diabetes* 2003;52:380–6.
15 Autio A, Uotila S, Kiugel M, *et al*. ^{68}Ga-DOTA chelate, a novel imaging agent for assessment of myocardial perfusion and infarction detection in a rodent model. *J Nucl Cardiol* 2020;27:891–8.
16 Sander CY, Mandeville JB, Wey H-Y, *et al*. Effects of flow changes on radiotracer binding: simultaneous measurement of neuroreceptor binding and cerebral blood flow modulation. *J Cereb Blood Flow Metab* 2019;39:131–46.
17 Sauleau P, Lapouble E, Val-Laillet D, *et al*. The pig model in brain imaging and neurosurgery. *Animal* 2009;3:1138–51.
18 Eriksson O, Rosenström U, Selvaraju RK, *et al*. Species differences in pancreatic binding of DO3A-VS-Cys^{40}-Exendin4. *Acta Diabetol* 2017;54:1039–45.
19 Malbert C-H, Horowitz M, Young RL. Low-calorie sweeteners augment tissue-specific insulin sensitivity in a large animal model of obesity. *Eur J Nucl Med Mol Imaging* 2019;46:2380–91.
20 Bahri S, Horowitz M, Malbert C-H. Inward glucose transfer accounts for insulin-dependent increase in brain glucose metabolism associated with diet-induced obesity. *Obesity* 2018;26:1322–31.
21 Val-Laillet D, Blat S, Louveau I, *et al*. A computed tomography scan application to evaluate adiposity in a minipig model of human obesity. *Br J Nutr* 2010;104:1719–28.
22 Malbert C-H, Picq C, Divoux J-L, *et al*. Obesity-associated alterations in glucose metabolism are reversed by chronic bilateral stimulation of the abdominal vagus nerve. *Diabetes* 2017;66:848–57.
23 Selvaraju RK, Velikyan I, Johansson L, *et al*. In vivo imaging of the glucagonlike peptide 1 receptor in the pancreas with 68Ga-labeled DO3A-exendin-4. *J Nucl Med* 2013;54:1458–63.
24 Munk OL, Keiding S, Bass L. A method to estimate dispersion in sampling catheters and to calculate dispersion-free blood time–activity curves. *Med Phys* 2008;35:3471–81.
25 Malbert C-H. AniMate—an open source software for absolute PET quantification. *Annual Congress of the European Association of Nuclear Medicine* 2016.
26 Bettinardi V, Castiglioni I, De Bernardi E, *et al*. PET quantification: strategies for partial volume correction. *Clin Transl Imaging* 2014;2:199–218.
27 Innis RB, Cunningham VJ, Delforge J, *et al*. Consensus nomenclature for in vivo imaging of reversibly binding radioligands. *J Cereb Blood Flow Metab* 2007;27:1533–9.
28 Pyke C, Heller RS, Kirk RK, *et al*. Glp-1 receptor localization in monkey and human tissue: novel distribution revealed with extensively validated monoclonal antibody. *Endocrinology* 2014;155:1280–90.
29 Velasco C, Mateo J, Santos A, *et al*. Assessment of regional pulmonary blood flow using ^{68}Ga-DOTA PET. *EJNMMI Res* 2017;7:7.
30 Autio A, Saraste A, Kudomi N, *et al*. Assessment of blood flow with (68)Ga-DOTA PET in experimental inflammation: a validation study using (15)O-water. *Am J Nucl Med Mol Imaging* 2014;4:571–9.
31 Davids CR. Monitoring various eluate characteristics of the iThemba Labs SnO2-based 68Ge/68Ga generator over time and validation of quality control methods for the radiochemical purity assessment of 68Ga-labelled DOTA peptide formulations. *Master of Science in Nuclear Medicine* 2017.
32 Velasco C, Mota-Cobián A, Mota RA, *et al*. Quantitative assessment of myocardial blood flow and extracellular volume fraction using ^{68}Ga-DOTA-PET: a feasibility and validation study in large animals. *J Nucl Cardiol* 2020;27:1249–60.
33 Meier JJ, Gallwitz B, Salmen S, *et al*. Normalization of glucose concentrations and deceleration of gastric emptying after solid meals during intravenous glucagon-like peptide 1 in patients with type 2 diabetes. *J Clin Endocrinol Metab* 2003;88:2719–25.
34 Keramida G, Gregg S, Peters AM. Intrahepatic fluorine-18-fluorodeoxyglucose kinetics measured by least squares nonlinear computer modelling and Gjedde-Patlak-Rutland graphical analysis. *Nucl Med Commun* 2019;40:675–83.
35 Kim SY, Kim H, Cho JY, *et al*. Quantitative assessment of pancreatic fat by using unenhanced CT: pathologic correlation and clinical implications. *Radiology* 2014;271:104–12.
36 Ricci C, Longo R, Gioulis E, *et al*. Noninvasive in vivo quantitative assessment of fat content in human liver. *J Hepatol* 1997;27:108–13.
37 Tomas A, Jones B, Leech C. New insights into beta-cell GLP-1 receptor and cAMP signaling. *J Mol Biol* 2020;432:1347–66.
38 Duca FA, Sakar Y, Covasa M. Combination of obesity and high-fat feeding diminishes sensitivity to GLP-1R agonist exendin-4. *Diabetes* 2013;62:2410–5.
39 Yang M, Wang J, Wu S, *et al*. Duodenal GLP-1 signaling regulates hepatic glucose production through a PKC-δ-dependent neurocircuitry. *Cell Death Dis* 2017;8:e2609.
40 Bang-Berthelsen CH, Holm TL, Pyke C, *et al*. Glp-1 induces barrier protective expression in Brunner's glands and regulates colonic inflammation. *Inflamm Bowel Dis* 2016;22:2078–97.
41 Tanaka T, Nabatame H, Tanifuji Y. Insulin secretion and glucose utilization are impaired under general anesthesia with sevoflurane as well as isoflurane in a concentration-independent manner. *J Anesth* 2005;19:277–81.
42 Schirra J, Houck P, Wank U, *et al*. Effects of glucagon-like peptide-1(7-36)amide on antro-pyloro-duodenal motility in the interdigestive state and with duodenal lipid perfusion in humans. *Gut* 2000;46:622–31.
43 Honka H, Hannukainen JC, Tarkia M, *et al*. Pancreatic metabolism, blood flow, and β-cell function in obese humans. *J Clin Endocrinol Metab* 2014;99:E981–90.
44 Frayn KN, Karpe F. Regulation of human subcutaneous adipose tissue blood flow. *Int J Obes* 2014;38:1019–26.
45 Bagger JI, Knop FK, Lund A, *et al*. Glucagon responses to increasing oral loads of glucose and corresponding isoglycaemic intravenous glucose infusions in patients with type 2 diabetes and healthy individuals. *Diabetologia* 2014;57:1720–5.
46 Knop FK, Vilsbøll T, Højberg PV, *et al*. Reduced incretin effect in type 2 diabetes: cause or consequence of the diabetic state? *Diabetes* 2007;56:1951–9.
47 Nalin L, Selvaraju RK, Velikyan I, *et al*. Positron emission tomography imaging of the glucagon-like peptide-1 receptor in healthy and streptozotocin-induced diabetic pigs. *Eur J Nucl Med Mol Imaging* 2014;41:1800–10.
48 Heller RS, Kieffer TJ, Habener JF. Insulinotropic glucagon-like peptide I receptor expression in glucagon-producing alpha-cells of the rat endocrine pancreas. *Diabetes* 1997;46:785–91.